Journal of Environmental Chemical Engineering 13 (2025) 117324

Contents lists available at ScienceDirect

Journal of Environmental Chemical Engineering

journal homepage: www.elsevier.com/locate/jece

Optimizing the composition of bioactive coatings to support toluene removal

Javier González-Martín [a,b], Aránzazu del Campo [c], Raúl Muñoz [a,b], Raquel Lebrero [a,b,*]

[a] Institute of Sustainable Processes, University of Valladolid, Dr. Mergelina s/n., Valladolid 47011, Spain
[b] Department of Chemical Engineering and Environmental Technology, University of Valladolid, Dr. Mergelina s/n., Valladolid 47011, Spain
[c] INM - Leibniz Institute for New Materials, Campus D2 2, Saarbrücken 66123, Germany

ARTICLE INFO

Keywords:
Bioactive coating
Biofilm
Gas treatment
HNT
Latex
VOCs

ABSTRACT

The potential of bioactive coatings as an innovative biotechnology to overcome the mass-transfer limitations of conventional technologies when treating air pollutants, especially hydrophobic volatile organic compounds, was herein assessed. Bioactive coatings consist of active microorganisms entrapped in a polymer matrix, which needs to be porous to facilitate an effective gas pollutant exchange. To increase porosity, two additives, sucrose and glycerol mixtures (Suc/Gly) and halloysite nanotubes (HNTs), were included in the bioactive coatings at two concentration levels. The toluene removals of the different bioactive coatings were studied in batch mode at low (~300 mg m^{-3}) and high (~3000 mg m^{-3}) toluene concentrations. Overall, low HNTs concentration coatings supported optimum toluene removals (>95 %), comparable to biofilm controls at both toluene concentrations. High HNTs concentration coatings and low Suc/Gly concentration coatings achieved toluene removals over 95 % after 7 toluene injections at low toluene concentration. At high toluene concentrations, these coatings eventually outperformed the biofilm controls. High Suc/Gly concentration coatings supported a limited toluene removal (4 and 1 injection at low and high toluene concentrations, respectively), attributed to a preferential consumption of sucrose over toluene. These findings were corroborated by ESEM/conventional SEM imaging, revealing porosity in the HNTs bioactive coatings, visible at both the surface and internal levels. On the contrary, more homogeneous surfaces were observed in the Suc/Gly bioactive coatings, where total polymer coalescence was partially hindered by the addition of Suc/Gly. These results paved the way towards the implementation of bioactive coating in larger bioreactors for real-life air purification.

1. Introduction

Air pollution is nowadays one of the most important threats to both the environment and human health [1,2]. Numerous diseases have been attributed to air pollution, causing millions of premature deaths every year due to mortal illnesses such as acute lower respiratory/pulmonary diseases, ischemic heart disease or cancer. It is also responsible for other less severe health conditions, including allergies, asthma and various irritations [3,4]. Volatile organic compounds (VOCs), such as formaldehyde, toluene or limonene, are major contributors to air pollution. These compounds, often responsible for malodor episodes, are typically emitted at low concentrations in waste treatment facilities, animal farms or paper or mill industries [5]. In addition, VOCs are extensively used as solvents and chemical precursors in various industrial sectors, such as petrochemical or wood manufacturing, where they can lead to high-concentrated end-of-the-pipe emissions [6,7]. The control of these VOC-polluted airstreams has traditionally relied on physical-chemical air purification technologies. However, despite their widespread use, these technologies have notable drawbacks, including high energy consumption, substantial investment and operating costs, and the generation of secondary pollution [8,9].

Biotechnologies have already been explored for the treatment of industrial off-gases and other VOC emissions, where pollutants are typically limited in number and present at relatively stable concentrations, simplifying the biodegradation process [6,10,11]. However, the effective elimination of VOCs can be hindered when treating a wide

* Corresponding author at: Department of Chemical Engineering and Environmental Technology, University of Valladolid, Dr. Mergelina s/n., Valladolid 47011, Spain.
E-mail addresses: javier.gonzalezm@uva.es (J. González-Martín), aranzazu.delcampo@leibniz-inm.de (A. del Campo), mutora@iq.uva.es (R. Muñoz), raquel.lebrero@uva.es (R. Lebrero).

https://doi.org/10.1016/j.jece.2025.117324
Received 30 January 2025; Received in revised form 22 May 2025; Accepted 27 May 2025
Available online 29 May 2025

variety of VOCs or highly hydrophobic pollutants, such as in wastewater treatment plants or organic waste recycling facilities. Hence, the development of innovative biotechnologies aimed at enhancing the mass transfer of VOCs from the gas phase to microorganisms becomes imperative [12]. Some biological-based promising alternatives have already been explored, including the engineering of membrane [13] or capillary-based bioreactors [14]. However, membrane bioreactors remain economically unviable, and operational problems such as excessive biomass growth and clogging of the system limit their implementation. Similarly, capillary bioreactors still in the early stages of development and face challenges such as sustaining long-term operation and maintaining robust Taylor flow patterns, potentially impacting their performance [6,9].

In this paper, bioactive coatings are proposed as an innovative alternative to overcome typical VOC mass transfer challenges and bioreactor compactness. A bioactive coating is composed of a thin layer of a porous polymer that embeds a metabolically active microbial community. The microorganisms are embedded in a non-growing state, preventing the natural formation of a biofilm, which typically presents a high water content [15,16]. In the biodegradation process, the main challenge often consists of the transfer of the gas-phase pollutants to the liquid phase or water-rich biofilm. By using bioactive coatings, the hydrophobic compounds are directly transferred from the gas phase to the microorganisms. Therefore, the mass transfer is enhanced by avoiding the transport of the compounds through the water phase of the biofilm. Gas pollutants and water/nutrients can reach the microorganisms through the pores of the polymeric structure. Additionally, bioactive coatings can support high cell densities of microorganisms and have the potential to be implemented in different support materials and bioreactor configurations [16–18]. These characteristics also increase the potential of bioactive coatings for the design of more compact bioreactors that further intensify the biodegradation process.

Some small-scale applications of bioactive coatings have been developed. For instance, Gosse and Flickinger [19] proposed a method for bioactive coating preparation from latex (Rhoplex SF-012 or comparable), microorganisms and sucrose and glycerol as porogens, which has been used for the production of H_2 by immobilized *Rhodopseudomonas palustris* [20] or for the photosynthetic production of O_2 by immobilized cyanobacteria [21]. Similarly, Estrada et al. [22] prepared *Pseudomonas putida* F1 bioactive coatings for the removal of toluene, achieving 10 × higher removal rates than those obtained in agarose-based biofilms. The performance of bioactive coatings on different packing materials, namely expanded clay and polyurethane foam, was also evaluated for the treatment of VOC mixtures in bioreactors using a VOC-degrading culture enriched from an activated sludge inoculum [23,24]. Despite the potential of bioactive coating-based bioreactors for air purification has been demonstrated, VOC removals did not clearly outperform those obtained in conventional biofilm-based bioreactors. Thus, the authors concluded that further optimization of the bioactive coating is essential to fully realize the potential benefits of bioactive coatings. To this aim, additives were selected to increase the porosity of the bioactive coating by arresting the film coalescence, enhancing the mass transfer and thus the VOC removal potential. Sucrose/glycerol mixtures and halloysite nanotubes (HNTs) were selected based on previous research that demonstrated their effectiveness in creating porosity within the bioactive coating matrix [19,25]. Sucrose and glycerol contribute to the formation of highly viscous, glassy structures during the drying process of bioactive coatings, protecting microorganisms while creating porosity within the coating [19]. Meanwhile, HNTs are non-film forming particles that aggregate during drying, further enhancing pore formation and creating channels within the structure [25,26].

In this work, bioactive coatings containing the VOC-degrading bacteria *Rhodococcus opacus* were prepared and their performance in the elimination of toluene was assessed in batch assays. The effect of different additives (Suc/Gly mixtures; HNTs) in the porosity of the film was evaluated in order to maximize the VOC mass transfer at two different concentrations of toluene.

2. Materials and methods

2.1. Chemicals

Toluene (CAS 108–88–3) was selected as a model VOC due to its moderate hydrophobicity and frequent occurrence in several types of waste gas emissions [27,28]. Moreover, toluene was selected over other hydrophobic VOCs as it is commonly used in biofiltration studies for VOC removal [29,30], allowing for an easy comparison with previous research on VOC biodegradation. The preparation and composition of the cultivation medium (M9 medium) is described in Supplementary Materials. After preparation, M9 medium was sterilized and supplied under sterile conditions. The commercial emulsion PRIMAL™ SF-208 ER (acrylic-styrene copolymer; biocide and alkylphenol-ethoxylate free; MFFT ~4ºC; solids content 48.05 %; pH 8.0–9.5; Dow Chemical, Germany), kindly supplied by Brenntag Química (Barcelona, Spain), was selected for the preparation of the bioactive coatings. Toluene and glycerol were purchased from Panreac® (Barcelona, Spain), while D (+)-saccharose (sucrose) was purchased from Labkem (Barcelona, Spain). M9 medium components were obtained from both Labkem (Barcelona, Spain) and Panreac® (Barcelona, Spain). HNTs (Ø 30 −70 nm; length 1 −3 μm) were purchased from Sigma-Aldrich (Madrid, Spain).

2.2. Microorganisms

The bacterial strain *Rhodococcus opacus* (DSMZ Nº43205) was selected as model microorganism, based on the reported ability of the genus *Rhodococcus* to effectively biodegrade a large spectrum of organic compounds [31,32]. *R. opacus*, stored in DMSO at −80ºC, was reactivated and stored at 4ºC to be used afterwards as the stock culture.

For each experiment, a 100 mL bottle containing 20 mL of M9 medium was inoculated with 2 mL of the stock culture and cultivated for 24 h. The culture was then transferred to a 1.2 L bottle containing 200 mL of M9 medium and incubated for 24 h. The culture broth was then divided into four aliquots for the inoculation of four 1.2 L bottles containing 200 mL of M9 medium each, and then incubated for 24 h. The culture was centrifuged (7800 rpm, 10 min), resuspended in glucose-free M9 medium (40 mL) and centrifuged again to remove the remaining glucose. The biomass was resuspended in 40 mL of glucose-free M9 medium and used for the inoculation of four 1.2 L bottles containing 200 mL of glucose-free M9 medium. Finally, 5.5 μL of toluene were injected in each bottle as the sole carbon and energy source in order to acclimatize the microorganisms to toluene degradation. Toluene was supplemented to the headspace upon its depletion for a period of 7 days (resulting in a total of 10–12 injections). All cultivations were conducted at 24 ± 2ºC using Variomag Poly15 stirring plates (Thermo Fisher Scientific, Spain). To prevent contamination of the inoculum, all the materials used for *R. opacus* cultivation, as well as those used for medium preparation, were sterilized. Accordingly, an sterile atmosphere was used during culture manipulation and bioactive coating preparation.

2.3. Screening of additive concentrations

A preliminary set of bacteria-free experiments was performed to identify the optimum concentration of additives. Stock solutions of sucrose (580 g L^{-1}), glycerol (100 % v/v) and HNTs (50 % w/w) were prepared in deionized water. Mixtures containing latex (1 mL) and additives at different concentrations were prepared by using deionized water and stock solutions. Final concentrations from 9.7 to 101.5 mg mL^{-1} for sucrose and 1–7.5 % for glycerol were tested as starting points for the optimization, as previously reported by Gosse and Flickinger [19]. Additionally, final concentrations of HNTs from 1.0 %

to 50 % were initially tested, following the methodology described by Chen et al. [25]. All coatings were prepared by pipetting 70 μL of each mixture into a polystyrene 24-well plate (Sigma-Aldrich, Spain), and then left until dry. Then, water was added to each well to evaluate the wet stability of the coatings after rehydration.

2.4. Bioactive coating preparation

For the preparation of *Rhodococcus opacus* bioactive coatings, the toluene-acclimated cultures, as explained in the last paragraph of Section 2.2, were centrifuged and resuspended twice in 40 mL of glucose-free M9 medium. The biomass was finally resuspended in up to 5 mL of glucose-free M9 medium, with the volume adjusted based on the optical density of each culture to ensure consistent biomass content across experiments. The biomass was then mixed with the corresponding additives and polymer according to Table S1. Stock solutions of the additives (sucrose at 250 g L^{-1}, glycerol at 50 % v/v and HNTs at 33 % w/w) were prepared by using glucose-free M9 medium. Each additive was tested at two concentrations: 13.2 % and 1.0 % for HNTs, and 50 mg mL^{-1} / 4 % and 10 mg mL^{-1} / 1 % for Suc/Gly, respectively. Sterile deionized water and glucose-free M9 medium were added to ensure the same concentration of nutrients in each formulation. The additives were mixed with 2400 μL of polymer and 1200 μL of microbial suspension. The positive controls consisted of conventional biofilms, where the polymer was replaced by sterile water. All mixtures were vortex mixed thoroughly prior use.

The bioactive coatings were prepared by pipetting and uniformly distributing 800 μL of the mixture over the surface of an autoclaved filter paper (2 cm × 10 cm). The fresh bioactive coatings were dried at room temperature for 50–60 min in the laminar flow hood prior use. Uncoated, sterile filter paper was used as abiotic control. This systematic preparation procedure reduced the variability of the results due to experimental conditions.

2.5. Experimental procedure

Small-scale batch tests were designed to assess the toluene removal capacity of different bioactive coatings. Given that the study aimed to optimize the coating composition rather than assess its subsequent application, this simplified experimental approach provided flexibility and enabled rapid test performance. On the contrary, limitations regarding the application of bioactive coatings in larger scale systems need to be addressed in further work.

Two preliminary experiments were necessary to develop a robust setup. In the first preliminary test (PT1), all four bioactive coating compositions, abiotic controls and biofilms were tested in duplicate at low toluene concentration (~300 mg m^{-3}). In the second preliminary test (PT2), the setup was simplified and only one bioactive coating composition, i.e. the high HNTs concentration, was tested. Biofilms and bioactive coatings were prepared in triplicate, alongside an abiotic control in duplicate. The toluene removal efficiency was evaluated at high and low toluene concentrations (~3000 and ~300 mg m^{-3}, respectively). Additionally, 200 μL of glucose-free M9 medium were added in each bottle to overcome any possible water/nutrient limitation. In both experiments, toluene was periodically monitored and replenished when depleted. Finally, in the optimized experimental setup, a 3 cm × 11 cm autoclaved kitchen dishcloth piece was used as bioactive coating support and water-nutrient reservoir. The dishcloth was introduced in the bottle and the coating was placed onto it. Then, the dishcloth was impregnated with 2 mL of glucose-free M9 medium before sealing the bottle and injecting toluene. A schematic representation and a picture of the bioactive coating is shown in Fig. S1 A and B, respectively.

With this definitive experimental setup, four test series were performed to evaluate the bioactive coating compositions specified in Table S1. Each test series consisted of 16 bottles, with triplicates of conventional biofilms and bioactive coatings, and duplicates of abiotic controls. The bioactive coatings were introduced in sterile 1.2 L gas-tight bottles, sealed with 20 mm butyl stoppers (Supelco, USA). The assays were performed simultaneously at low and high toluene concentrations. A picture of the final experimental setup and the flowchart describing the experiments is shown in Fig. S1 C and D. The low toluene concentration was obtained by injecting 4.5 mL of a gaseous toluene standard with a 5 mL gas syringe (Hamilton, USA). The standard was freshly prepared by injecting 60 μL of toluene with a 100 μL liquid syringe (SGE 100R-GT-LC, Australia) in a 500 mL glass bulb (Sigma-Aldrich, Spain). The high toluene concentration was achieved by directly injecting 5.5 μL of liquid toluene into the gas-tight bottles with a 10 μL micro syringe (Gastight 1801RN, Hamilton, USA). Toluene consumption was followed by measuring its gas-phase concentration by GC-FID. When depleted in the three replicates, toluene was replenished in the bottles to the selected concentration following the procedure described above. To evaluate the robustness of the bioactive coatings, two starvation periods (~72 h) were performed in each experiment.

2.6. Analytical procedures

Toluene concentration was measured by GC-FID. Toluene was sampled from each bottle with a 250 μL gastight syringe (Hamilton, USA), and measured by using an Agilent 8860 gas chromatograph (USA), equipped with an Agilent HP-5 19091J-413 capillary column (30 m × 0.32 mm × 0.25 μm) and an FID (flame ionization detector). Injector and detector temperatures were set at 150 and 250ºC, respectively. The oven temperature was fixed at 80ºC for 2.5 min and then increased to 150ºC at a 100ºC min^{-1} rate. Helium was used as carrier gas (2.0 mL min^{-1}). FID flowrates were set at 30 mL min^{-1} for hydrogen, 400 mL min^{-1} for air and 25 mL min^{-1} for nitrogen as the make-up gas. External standards of toluene were used for calibration.

Scanning Electron Microscopy (SEM) was used to study the surface of bioactive coatings and investigate the effect of additive concentration on its structure. Environmental SEM (ESEM) was also used due to the simplicity of sample preparation and analysis that allows minimum surface alterations. For SEM imaging, bioactive coatings were prepared as described in Section 2.4. A representative portion of each bioactive coating was placed on an aluminum stub using double-sided carbon tape. ESEM samples were analyzed with no further treatment, whereas for conventional SEM, samples were gold-coated (15 nm) with an Emitech K575XD Turbo-Pumped Sputter Coater before analysis. A QUANTA 200 FEG SEM was used for imaging. Electron beam voltage was set at 5 keV for ESEM and 5–20 keV for conventional SEM.

2.7. Data treatment

Removal efficiency (%RE) was calculated comparing toluene concentration measurements as described in Eq. 1:

$$\%RE = 100 \times \left(1 - \left(\frac{Ct_i}{Cin_i}\right)\right) \quad (1)$$

where Cin_i is the initial toluene concentration of each injection i and Ct_i is the concentration of toluene at a time t, both given in mg m^{-3}.

Toluene removal rate (mg m^{-2} h^{-1}) was calculated for each injection of toluene, as described in Eq. 2:

$$R = \left(\frac{Cin_i - Ct_i}{t_i - t_0}\right) * \frac{V}{A} \quad (2)$$

where t_0 represents the initial time of each injection, t_i the time at which the concentration Ct_i was measured, V represents the volume of the bottle (0.0012 m^3), and A represents the surface of the bioactive coating (0.002 m^2). Units of both t_o and t_i are given in h.

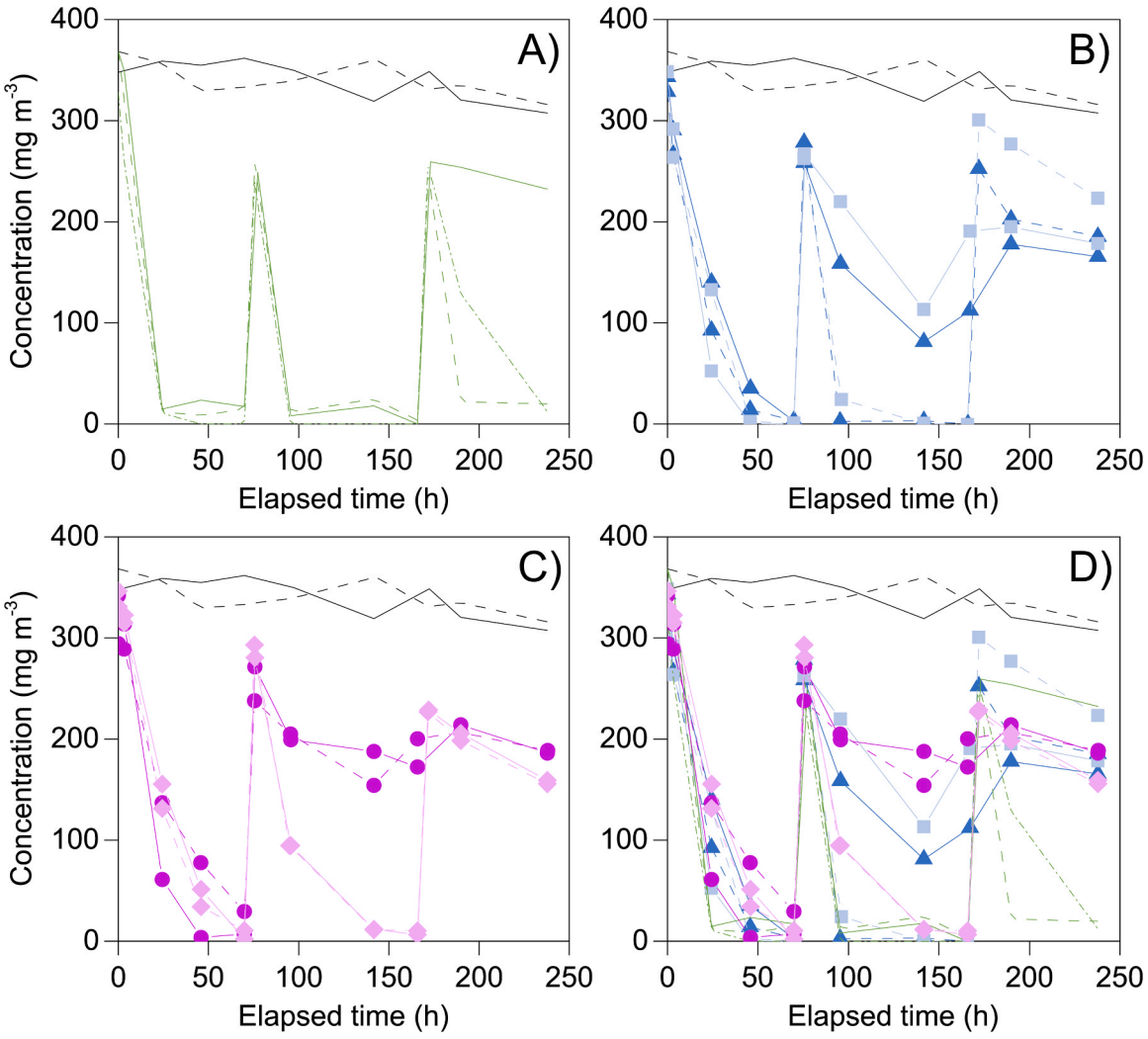

Fig. 1. Time course of toluene concentrations during preliminary test PT1 in A) biofilm controls (——/– – –/– · –), B) bioactive coatings with high (▲—/▲– –) and low (■—/■– –) concentration of HNTs, C) bioactive coatings with high (●—/●– –) and low (◆—/◆– –) concentration of Suc/Gly. Black lines represent the abiotic controls (——/– – –). Fig. D shows the comparative evolution of toluene concentration in all the bottles.

3. Results and discussion

3.1. Screening of additive concentrations

Bioactive coatings at the highest Suc/Gly concentrations, i.e. 101.5 mg mL^{-1} and 7.5 % as reported in Gosse and Flickinger [19], were shown to be unstable when water was added, which is an essential requirement for the implementation of bioactive coatings for biofiltration. Therefore, a new assay was conducted with lower concentrations of sucrose and glycerol (9.7, 29.0 and 77.3 mg mL^{-1} of sucrose; 1.0 and 4.0 % of glycerol), for a total of six samples. As shown in Fig. S2, some coatings exhibited a whitening effect after hydration, particularly around the periphery. These coatings retained their mechanical stability, and only sample S6, (maximum concentrations of Suc/Gly) redissolved after rehydration. Wet stability increased when the concentration of additives decreased. As porosity increases with additive concentration, a compromise to maximize porosity is needed while retaining wet stability. Therefore, sucrose concentration was reduced to 50.0 mg mL^{-1} to ensure their mechanical stability after rehydration. Thus, for the experiments with bacteria, maximum concentrations were set at 50 mg mL^{-1} and 4 % for sucrose and glycerol. Minimum concentrations were established at 10 mg mL^{-1} and 1 %, respectively.

This problem was not observed in coatings with HNTs as additive. Formulations with up to 25 % w/w of HNTs formed stable coatings. However, further experiments at this high HNTs concentration (data not shown) demonstrated poor attachment, as cell outgrowth was observed. To avoid cell leakage, HNTs concentrations below 13.2 % were used, while the minimum concentration was set at 1.0 %.

3.2. Toluene removal performance in preliminary tests (PT1 and PT2)

The toluene removal efficiency during PT1 is shown in Fig. 1. Certain issues were identified in this experiment that compromised the reliability of the results. First, an experimental setup including four different compositions of bioactive coatings involved long preparation periods. Indeed, a prolonged drying and starvation period may have a negative impact on the microorganisms, potentially leading to a reduced metabolic activity at the beginning of the experiment. Also, the drying period was different depending on each composition. Although this phenomenon was not observed in other bioactive coating experiments

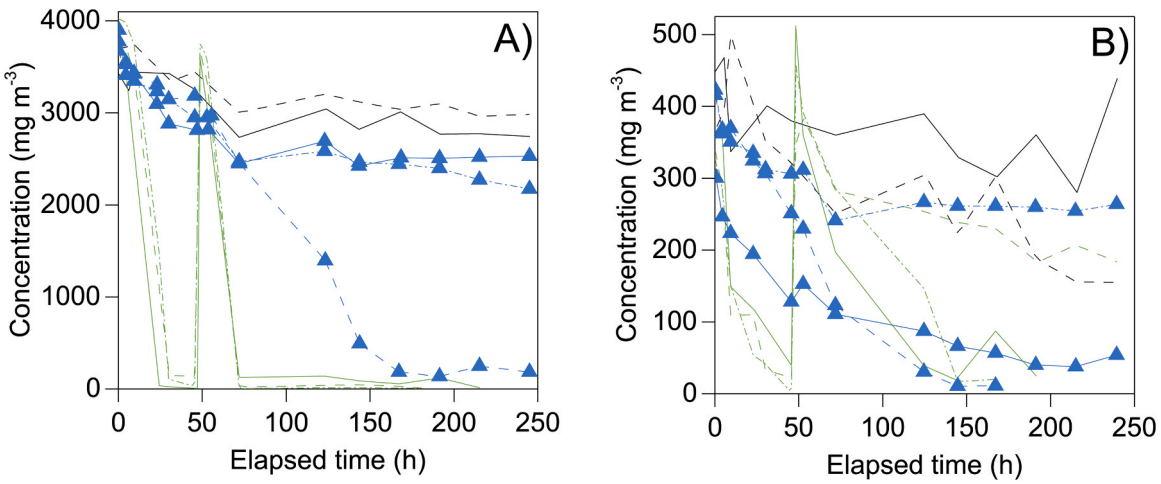

Fig. 2. Time course of toluene concentrations during preliminary test PT2 at A) high and B) low toluene concentrations, in coatings with high concentration of HNTs (▲/▲/▲), biofilms (——/– – –/– · –) and abiotic controls (——/– – –).

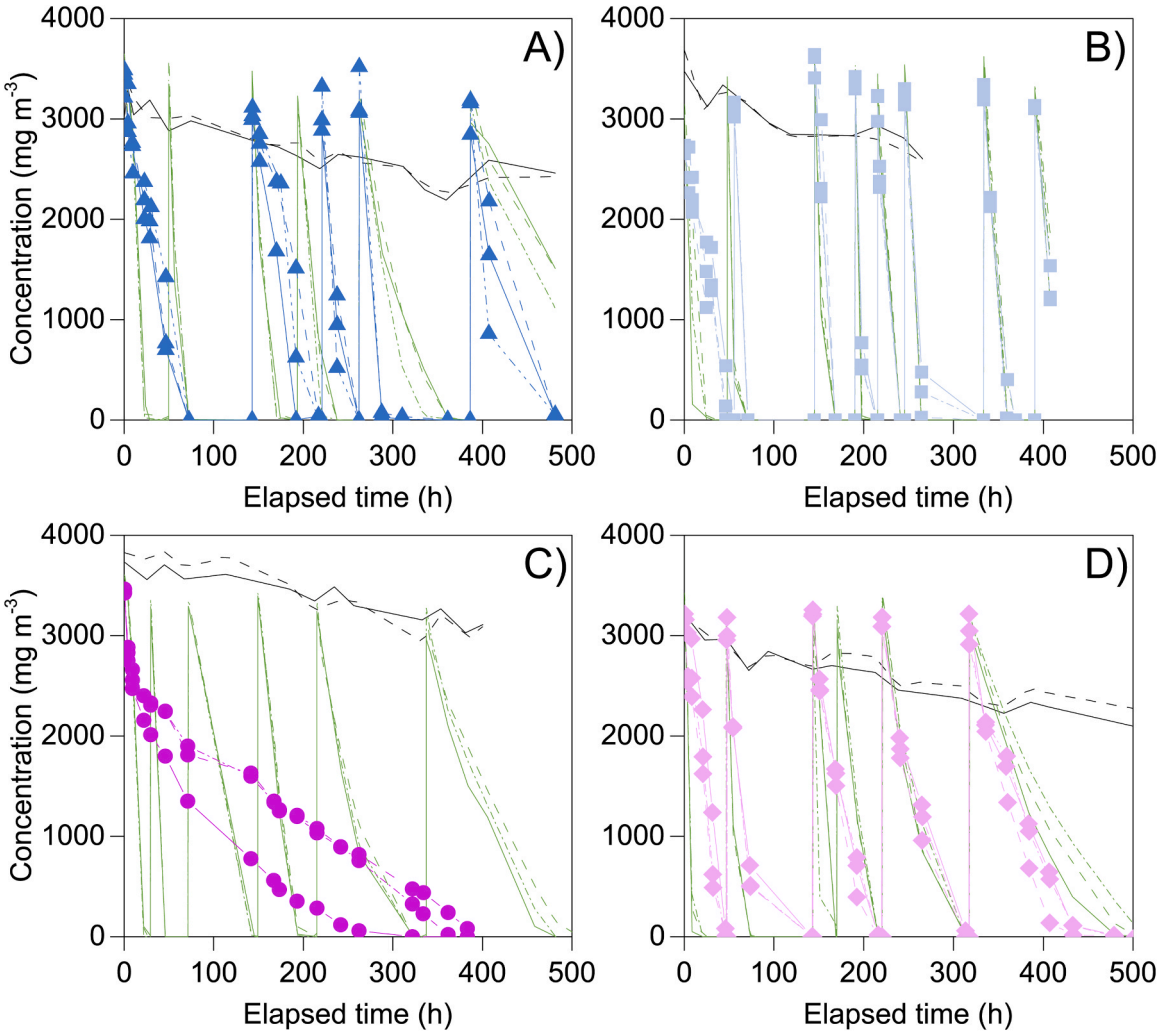

Fig. 3. Time course of toluene concentrations during the biodegradation experiments at high toluene concentration. Bioactive coatings with A) high HNTs concentration (▲/▲/▲), B) low HNTs concentration (■/■/■), C) high Suc/Gly concentration (●/●/●), and D) low Suc/Gly concentration (◆/◆/◆). All experiments included abiotic controls (——/– – –) and biofilm controls (——/– – –/– · –).

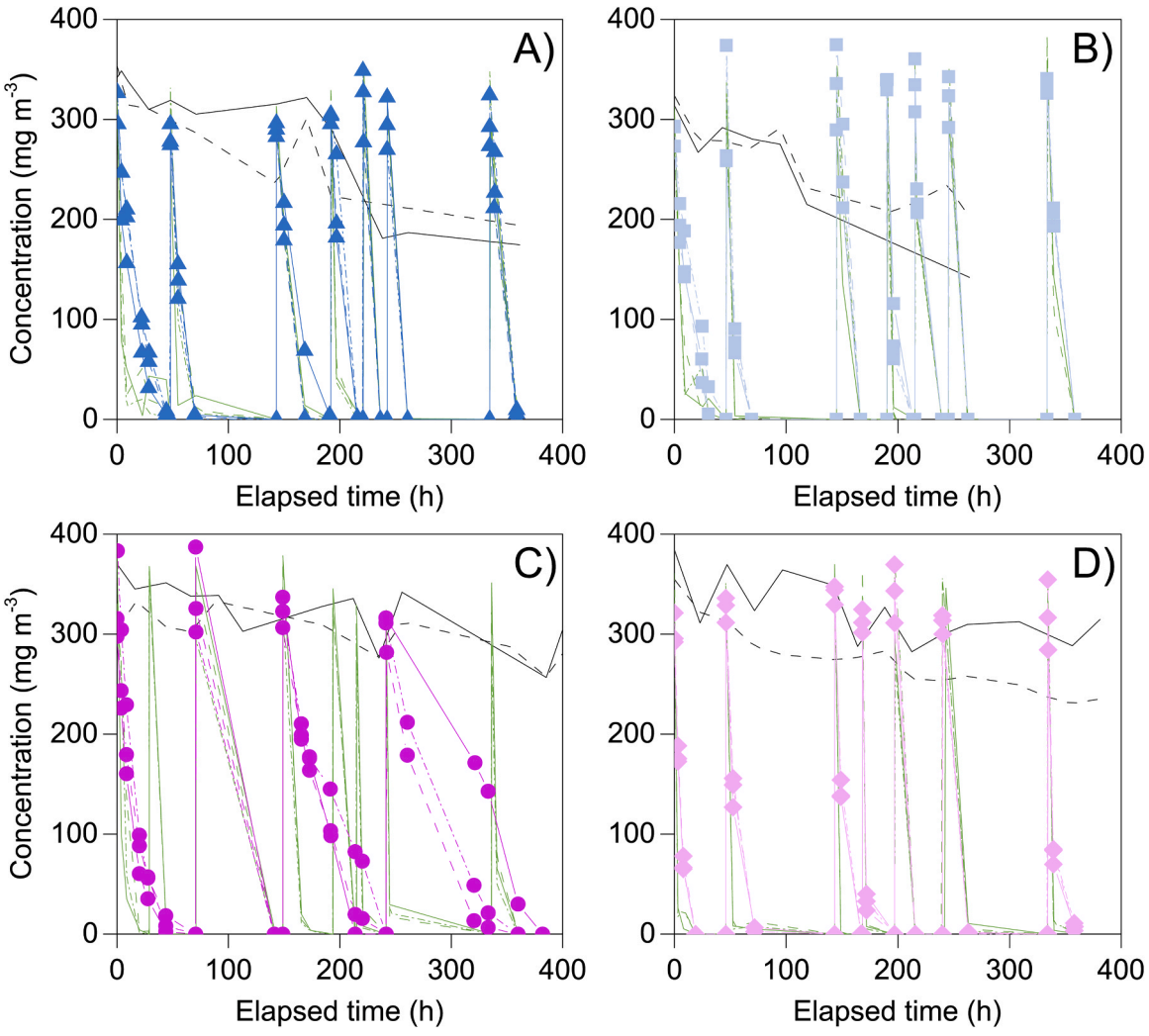

Fig. 4. Time course of toluene concentrations during the biodegradation experiments at low toluene concentrations. Bioactive coatings with A) high HNTs concentration (—▲—/- -▲- -/—▲— ·), B) low HNTs concentration (—■—/- -■- -/—■— ·), C) high Suc/Gly concentration (—●—/- -●- -/—●— ·), and D) low Suc/Gly concentration (—◆—/- -◆- -/—◆— ·). All experiments included abiotic controls (——/- - - -) and biofilm controls (——/- - - -/— · —).

where longer drying periods were used [33], the response of different microbial species to latex immobilization can vary significantly and remains largely unexplored [34]. Complete toluene removal was achieved by the biofilm controls after 24 h, while longer periods (45–70 h) were observed for HNTs and Suc/Gly coatings. After the second toluene addition, inconsistent results were observed, especially among duplicates with the same coating composition, which was attributed to insufficient water/nutrient levels necessary to sustain the microbial activity. This limitation likely arose during the drying process of the coatings, resulting in a reduced moisture/nutrient content. A similar issue was detected by Estrada et al. [22] when preparing latex coatings for toluene removal. Coatings that were not rehydrated only supported limited removal of toluene before experiencing a reduced microbial activity, while coatings continuously hydrated by capillarity through the supporting material achieved more than twice the elimination capacity (0.230 vs. 0.095 mg cm^{-2} h^{-1}). Similarly, air humidity has a strong effect on microorganism survival as reported by Xu et al. [35]. An increase in humidity from 40 % to 80 % promoted the growth rate of *Pseudomonas putida* F1 biofilms (28–73 mg $_{DCW}$ g^{-1}) when degrading 60 ppm_v of toluene.

Several setup modifications were implemented in PT2 to address the issues encountered in the previous experiment. Only one composition of bioactive coating was used, at both high and low toluene concentration. Likewise, glucose-free M9 medium was added before sealing the bottles to provide moisture and nutrients by capillarity, similar to other studies on paper-supported bioactive coatings [36,37]. Despite these improvements, the toluene removal performance was not consistent (Fig. 2).

At high toluene concentrations, HNT coatings were unable to completely remove toluene. At low concentrations, toluene removal was uneven among replicates. This variability was again attributed to an irregular drying during the experiment and further loss of microbial activity within the coatings by an insufficient water/nutrients supply or an uneven distribution within the supporting material. In response, a dishcloth piece was proposed as water/nutrient reservoir. This would allow a higher volume of glucose-free M9 medium in each bottle, absorbed by the dishcloth and continuously supplied by capillarity to the coating placed on top, thereby eliminating the variability in the drying process of the bioactive coatings. This configuration also frees the top surface of the coating for an effective gas transfer to the microorganisms, which is usually the main bottleneck for the treatment of

hydrophobic VOCs [38]. A similar approach was followed by In-na et al. [33], where the supporting material (loofah sponge) provided water and nutrients by capillarity while the cyanobacteria-based bioactive coating remained in contact with the gas phase. The challenges of water supply and nutrient limitations are expected to be mitigated in larger-scale bioreactors, where continuous, automated flow enables precise control over medium supply and medium replacement as needed.

3.3. Toluene removal performance at high toluene concentration

The experiments at high toluene concentrations with each bioactive coating composition are shown in Fig. 3. Toluene was injected at 3263 ± 206 mg m^{-3} (average of all injections). Toluene losses were observed in all abiotic controls, initially attributed to adsorption (occurring during the first hours of the experiment until surface saturation) and subsequently due to progressive diffusion through the bottle septum. Despite final toluene losses of up to 36 % were recorded after 360 h of assay (Fig. 3A), the abiotic controls were considered valid as the consumption of toluene by the bioactive coatings occurred at a significantly faster rate.

At first, all bioactive coatings removed toluene slower than their biofilm control counterparts. Biofilms completely consumed the first injection of toluene in less than 24 h (Fig. 3), whereas all latex-based coatings only achieved 30–50 % removal of toluene within that timeframe. Low HNTs concentration and low Suc/Gly concentration coatings removed toluene faster than high HNTs concentration coatings (<46 h vs. <72 h). Overall, the best toluene consumption performance was achieved by the low concentration HNTs coatings, which were able to completely remove 8 toluene injections, nearly replicating the results of the biofilm controls. On the contrary, high HNTs concentration coatings and low Suc/Gly concentration coatings initially exhibited a complete degradation of toluene but at a lower rate than their biofilm controls. This trend gradually shifted towards the opposite situation, where, after the last toluene injection, both high HNTs concentration and low Suc/Gly concentration coatings eventually removed toluene faster than their corresponding biofilms (Fig. 3A and D, respectively). This improvement suggests a progressive adaptation of the microbial community to the entrapment within the bioactive coating with a notably faster adaptation period observed in coatings with low HNTs concentration. Adaption phases are commonly reported in biofiltration processes, where microorganisms gradually adjust to their environment. In this case, the entrapment of the microorganisms within a bioactive coating may have prolonged this period by limiting the initial access to nutrients and gases, as well as modifying environmental conditions (i.e. drying period), thereby delaying full metabolic activity [23,24].

Although rapid toluene removal was observed at the beginning of the experiment, high Suc/Gly concentration coatings did not achieve complete toluene removal until 383 h of experiment (16 days). Thus, this composition of bioactive coating was considered inadequate, as the biofilm controls proved an excellent performance with complete removal of 6 injections of toluene (Fig. 3C). Wet coalescence following rehydration has been commonly observed in bioactive coatings containing sucrose. For example, Lyngberg et al. [39] reported a 50 % reduction in diffusivity after 5 days. However, the bioactive coating with a low Suc/Gly concentration achieved high toluene removals over the entire experiment, suggesting that wet coalescence was not the primary factor limiting toluene removal. Instead, the high sucrose content in the bioactive coating could have served as a more readily available carbon source for the microorganisms, hindering toluene consumption. Similarly, Xu et al. [35] observed an increased growth of *Pseudomonas putida* F1 biofilms when sucrose was added to LB medium, indicating preferential consumption of this compound even over other dissolved carbon sources. On the contrary, sucrose addition was not critical in other studies involving bioactive coatings, as this will depend on the specific microbial population [36].

3.4. Toluene removal performance at low toluene concentration

In this test series, toluene was supplemented at low concentration, with an average of 323 ± 30 mg m^{-3} (all injections). Similar to the previous experiments, toluene concentration progressively decreased in the abiotic controls throughout the experiments, with maximum losses of up to 54 % at 264 h of experiment (Fig. 4 B). The decrease in toluene concentration was mainly attributed to diffusion through the septum, although adsorption to the surfaces may have also played a role. Additionally, potential contamination of the abiotic controls cannot be ruled out, as the same gas syringe was used to periodically sample all bottles. Although the toluene removal rates in biofilms and bioactive coatings were significantly higher than those attributable to adsorption or diffusion effects, additional abiotic controls were conducted (Fig. S3). Toluene losses remained < 15 % were observed, confirming that physical and chemical effects on toluene removal were negligible compared to microbial degradation.

The behavior of biofilm controls and bioactive coatings followed a similar pattern to those observed with high toluene concentration (Fig. 4). After the first injection, toluene removal by biofilm controls was faster than that recorded in the bioactive coatings regardless of the composition. This delay in toluene removal by bioactive coatings can be attributed to a short activation period of the microorganisms following the drying of the latex coating, a process that either did not occur or was less pronounced in the case of biofilms. Lag periods at the initial stages of bioreactor operation are commonly reported, even when microorganisms previously acclimatized to the target pollutants are used [40,41]. Indeed, this lag period can be longer when using bioactive coatings, as microorganisms need to adapt to a new environment and more adverse operating conditions. In this context, González-Martín et al. [23,24] reported a similar behavior in VOC biofiltration studies, where the bioactive coating-based bioreactors experienced longer lag periods but progressively achieved similar removals than those of the biofilm-based bioreactors.

The coatings with high Suc/Gly concentration were again the worst performing composition compared with their corresponding biofilm controls. Again, it was hypothesized that the higher sucrose content in this coating provided a more accessible carbon source for microbial growth compared to the gas-phase toluene, resulting in a decrease in the rate of toluene removal compared with the low Suc/Gly concentration bioactive coatings. In contrast to the previous experiment, several toluene injections were completely consumed. Taking into account the total amount of toluene biodegraded, ≈ 4.8 mg were removed in 300–400 h in the high toluene concentration experiment. On the contrary, at low toluene concentrations, 4 injections containing ≈ 0.52 mg of toluene each were successfully biodegraded within 400 h. This represents a lower total amount of toluene biodegraded compared to the high concentration experiment.

Only minor differences were found among the rest of the bioactive coating compositions and their biofilm controls, both achieving a complete removal of 7 toluene injections. For example, shortly after the second injection (50 h approx.), high HNTs concentration bioactive coatings reached ~54 % removal, low HNTs concentration coatings achieved ~73 % and low Suc/Gly concentration coatings ~56 % after 8 h, while their biofilm counterparts exhibited removals of ~73, ~99 and ~98 %, respectively. On the other hand, the bioactive coatings responded successfully to the 72 h starving periods after the first and second weeks of each experiment. After these periods, biofilm controls maintained their previous toluene removal performance, while lower removal rates were recorded for the bioactive coatings. This effect can be clearly observed in Fig. 4D, in which the bioactive coatings required more time to reach a complete toluene removal (150 and 350 h). Additionally, toluene degradation rates, calculated with Eq. 2, were always slightly higher for the biofilm controls than for bioactive coatings. Even though these calculations depend on the time between measurements, biofilms exhibited maximum rates of 61.9 mg m^{-2} h^{-1},

Table 1
Absolute and average maximum removal rates (standard deviation), expressed in mg m^{-2} h^{-1}, achieved by the biofilms and the bioactive coatings throughout the experiments.

Bioactive coating composition	Sample	Absolute maximum removal rate	Averaged maximum removal rate (St. Dev.)
High HNTs Conc.	Bioactive coating	16.2	10.3 (2.5)
	Biofilm	34.8	17.0 (9.3)
Low HNTs Conc.	Bioactive coating	44.5	17.1 (10.0)
	Biofilm	49.6	23.6 (12.0)
High Suc/Gly Conc.	Bioactive coating	11.8	6.0 (4.2)
	Biofilm	55.1	24.2 (15.0)
Low Suc/Gly Conc.	Bioactive coating	44.9	20.5 (11.1)
	Biofilm	61.9	32.3 (17.6)

significantly higher than those observed for high and low HNTs concentration (16.2 and 44.5 mg m^{-2} h^{-1}) and high and low Suc/Gly concentration bioactive coatings (11.0 and 44.9 mg m^{-3} h^{-1}, respectively). Similarly, differences were observed in the average maximum elimination rates between biofilm controls and bioactive coatings (Table 1), calculated using the maximum degradation rate for each of the three replicates of biofilm controls or bioactive coating compositions during toluene injection.

3.5. Study of film morphology

The surface morphology of the bioactive coatings was examined by SEM and ESEM. Conventional SEM and ESEM each have different strengths and drawbacks, but when used together they can provide complementary information to obtain a more comprehensive understanding of the bioactive coating surface [42–44]. At low magnification (≤2000 ×), SEM and ESEM images did not show differences between similar samples. In both high and low HNTs concentration bioactive coatings (Fig. S5), some structures were observed, attributed to HNTs clusters on the surface of the coating. The surface of Suc/Gly bioactive coatings (Fig. S4) was more homogeneous and similar to a bioactive coating with no additives. In both images, it was possible to observe the loss of most of the natural macroporosity of the filter paper surface after the application of the bioactive coating, contrary to the biofilm controls, which clearly preserved this structure (Fig. S6). Although a very porous structure is generally beneficial due to the increase in active surface, this loss is not critical to pollutant mass transfer and the activity of the bioactive coating as long as microporosity is achieved. An increase in active surface should be assessed and discussed in further research.

At higher magnification (≥10000 ×), a blurry structure was observed by SEM in the biofilm control, reporting no useful information. Some structures were observed in ESEM analyses, but no cells were clearly detected (Fig. S6). This was attributed to the high water content,

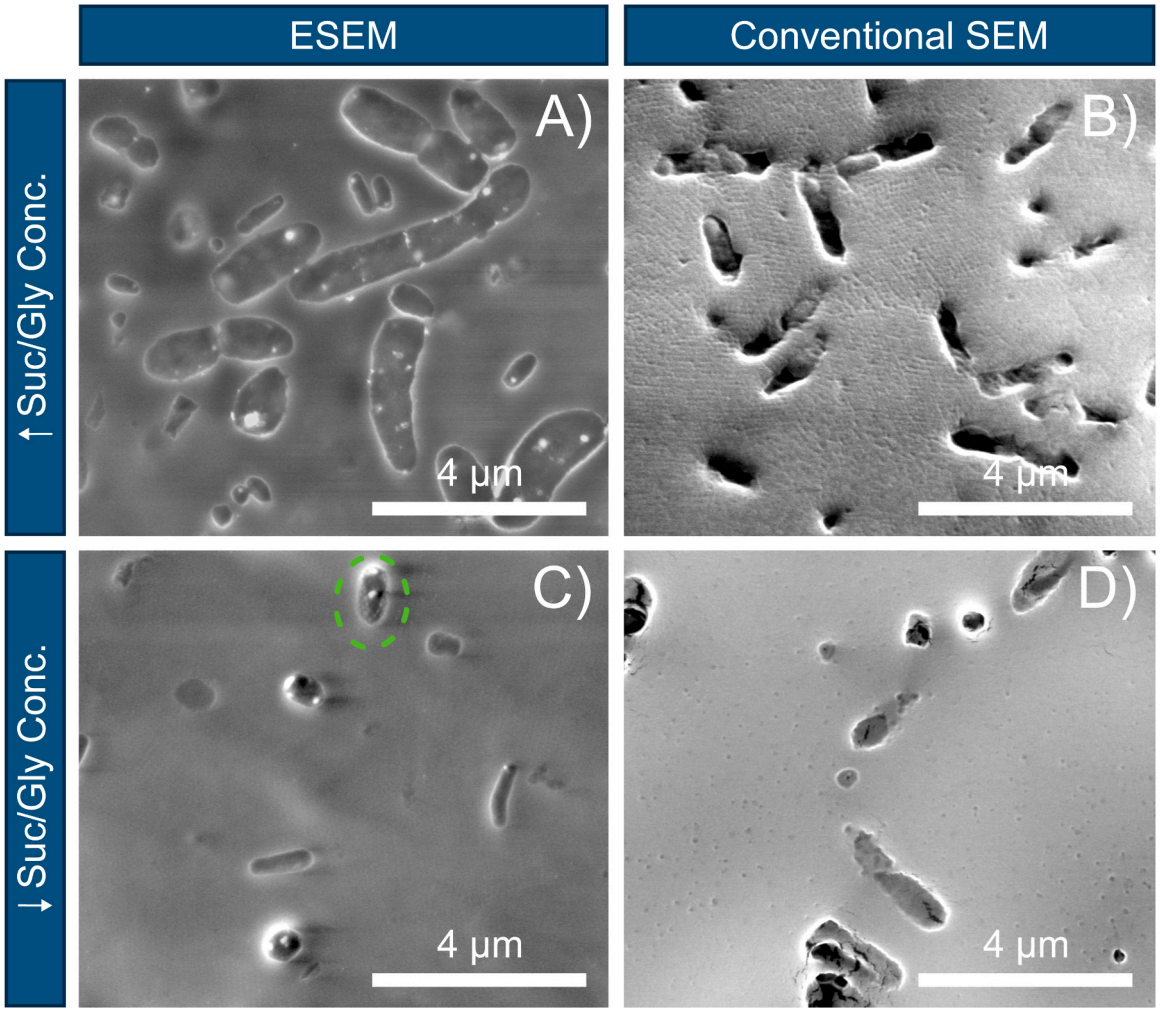

Fig. 5. ESEM and conventional SEM images of: A) and B) high Suc/Gly concentration bioactive coatings; and C) and D) low Suc/Gly concentration bioactive coatings.

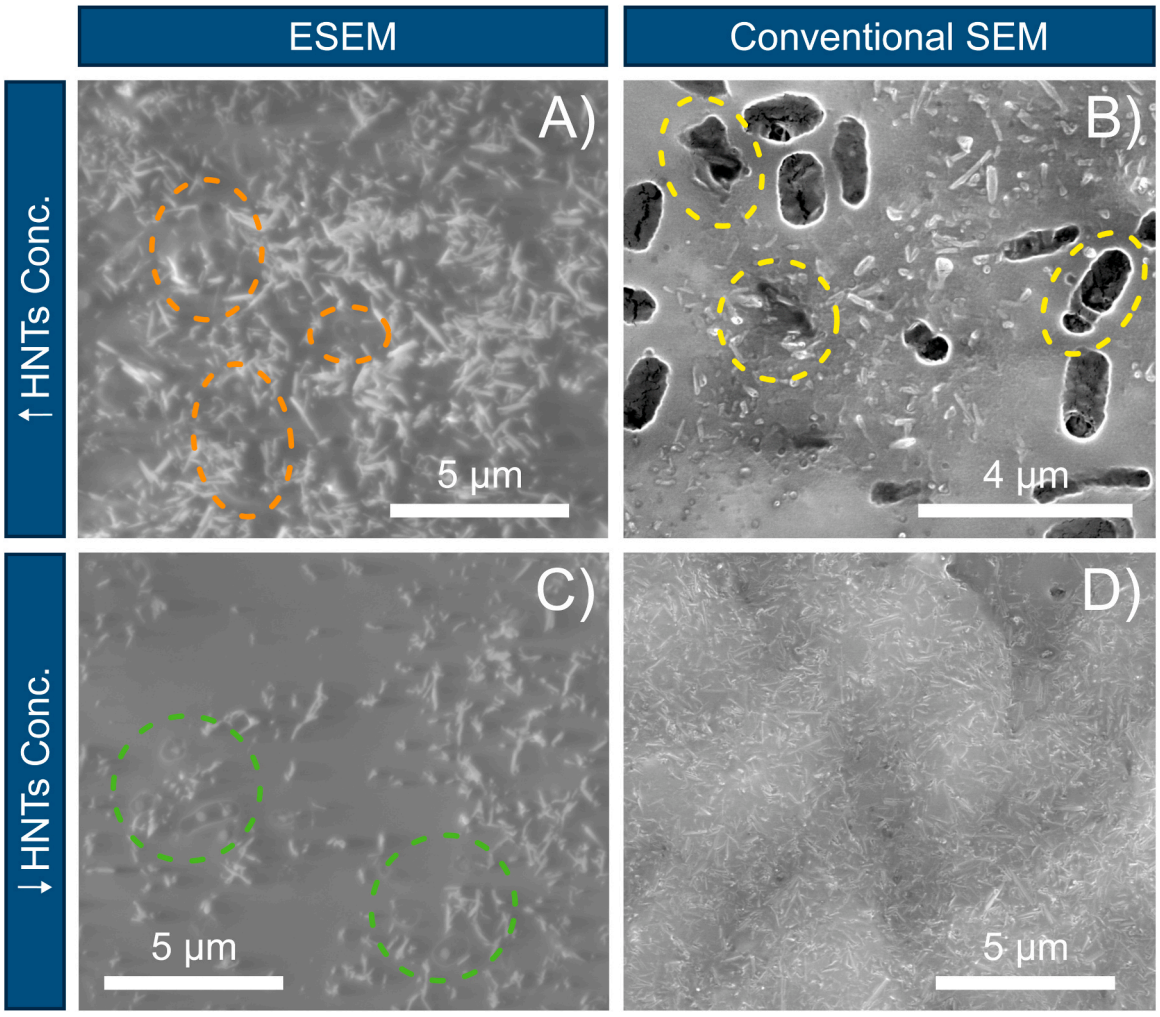

Fig. 6. ESEM and conventional SEM images of: A) and B) high HNTs concentration bioactive coatings; and C) and D) low HNTs concentration bioactive coatings.

which impeded an accurate visualization of the microorganisms [43]. Challenges in properly visualizing aqueous biofilms using ESEM have been previously reported. Although cryo-SEM is sometimes used to image samples with high water content, the freeze-drying process can create artificial pores and structures, which eventually could lead to misinterpretation of the structure [45]. On the contrary to conventional biofilms, bioactive coatings exhibited much less moisture on the surface, and therefore, some bacteria were detected in ESEM and conventional SEM images of Suc/Gly coatings, with a higher cell concentration for the high Suc/Gly coating (Fig. 5). Darker images were obtained by ESEM, as the electron beam quickly damaged the surface at high magnifications. Similar images were reported in the ESEM imaging of *Bacillus subtilis* [46]. Although noticeable in both images, bacteria were detected clearer in SEM by the voids left on the surface of the coating. Regarding the surface of the coating, the fine latex structure could be observed in the high Suc/Gly coating (Fig. 5 B), in which individual latex particles were deformed but total coalescence did not occur. In low Suc/Gly concentration coatings, coalescence seemed more extended, but some small pores also appeared along the surface. In agreement with Lyngberg et al. [39], higher osmoprotectant concentrations can prevent coalescence more extensively than low concentrations. Indeed, latex particles were also slightly detectable in Fig. 5C, both along the surface and also partially covering a cell. Nevertheless, despite the satisfactory porous structure observed, the preferential consumption of osmoprotectants may have limited further toluene removal, as explained in previous sections.

As observed in previous studies, HNTs were easily distinguishable in both ESEM and SEM (Fig. 6). The inorganic nature of HNTs, an aluminosilicate-based material, provides a sharper contrast compared to organic structures like latex, especially in ESEM. In agreement, ESEM images in our study offered a clearer view of the HNT distribution across the surface of the coating, which reflected the higher presence of HNTs in the high HNTs concentration bioactive coating. In addition, some cells were detected in the ESEM images of both HNTs concentration bioactive coatings (Fig. 6A and C). However, bacteria were not as clearly observed as in Suc/Gly coatings, which was attributed to this high contrast between the inorganic HNTs and the organic structures. In conventional SEM images, HNT structures in latex coatings similar to those reported in Chen et al. [25] and Qiao et al. [47] were observed. However, a more homogeneous surface of the HNTs bioactive coatings was recorded in this study, especially in the low HNTs concentration coating. Although lower concentrations of HNTs were herein used for the bioactive coatings, some porous areas were perceived in both high and low HNTs bioactive coatings. This could explain the great performance of HNT bioactive coatings during the toluene elimination experiments. More specifically, a deeper porous structure was revealed in the void spaces left by missing bacteria (Fig. 6 B), which could indicate that the gas-phase pollutants can be transferred to the bacteria inside the bioactive coatings, and also moisture and nutrients from the supporting material can reach the cells on the surface of the coating. Additionally, the hollow structure of HNTs (Ø~50 nm) allows the passage of small molecules, which could have also benefited an effective transport. This

fact was in agreement with previous research on bioactive coatings, in which one side of the coating is exposed to the gas-phase pollutants and the opposite side is in contact with a porous supporting material that provides moisture and nutrients [22,36].

4. Conclusions

In this study, different compositions of bioactive coatings were explored and their effectiveness in toluene removal was compared to that of conventional biofilms. Toluene removal was significantly influenced by the type and concentration of additives and the resulting microstructure inside the bioactive coating. Biofilm controls consistently demonstrated rapid and complete toluene removal, usually within 24 h. Low HNTs concentration bioactive coatings closely matched the biofilm control performance at both toluene concentrations. At high toluene concentrations, high HNTs concentration coatings and low Suc/Gly concentration coatings eventually outperformed biofilm controls, indicating adaptation over time. At low toluene concentrations, these coatings nearly replicated the performance of biofilm controls. Toluene removal by high Suc/Gly concentration coatings was generally very limited, attributed to the preferential consumption of the readily available sucrose over gas-phase toluene.

ESEM and conventional SEM imaging revealed microstructures in alignment with toluene removals. Although bacteria were difficult to detect, porous structures were observed in HNTs coatings. Bacteria were easily observed in Suc/Gly bioactive coatings, with distinct latex particles detected on the surface of Suc/Gly coatings and also covering some bacteria. This observation suggests a stopped coalescence process, crucial for enhancing porosity and therefore microbial activity. These structural observations demonstrate the critical role of additive concentration and coating microstructure in optimizing bioactive coatings for VOC removal.

Overall, the bioactive coating with a low concentration of HNTs demonstrated the best performance among the different bioactive coating compositions, achieving the highest and fastest toluene removal at both tested concentrations. This suggests its potential for scaling up in technological applications. Future steps involving continuous lab-scale bioreactor experiments based on the bioactive coating model herein studied to evaluate the long-term toluene removal performance are necessary.

CRediT authorship contribution statement

Raquel Lebrero: Writing – review & editing, Supervision, Project administration, Funding acquisition, Conceptualization. **Raúl Muñoz:** Writing – review & editing, Supervision, Project administration, Funding acquisition, Conceptualization. **Javier González-Martín:** Writing – review & editing, Writing – original draft, Visualization, Investigation, Formal analysis, Conceptualization. **Aránzazu del Campo:** Writing – review & editing, Supervision.

Declaration of Competing Interest

The authors declare that they have no known competing financial interests or personal relationships that could have appeared to influence the work reported in this paper.

Acknowledgements

This work was supported by the Ministry of Science, Innovation and Universities [project RTI2018–0–096441-B-I00]. The Regional Government of Castilla y León and the EU-FEDER program [UIC 393, UIC 379] are also gratefully acknowledged. The financial support of the Regional Government of Castilla y León (Consejería de Educación) and the European Social Fund is also acknowledged for the PhD grant of J. González-Martín (BDNS 487971).

Appendix A. Supporting information

Supplementary data associated with this article can be found in the online version at doi:10.1016/j.jece.2025.117324.

Data Availability

Data will be made available on request.

References

[1] European Environment Agency, Europe's air quality status 2023, 2023. ⟨https://doi.org/10.2800/59526⟩.
[2] World Health Organization, WHO global air quality guidelines. Particulate matter (₱PM2.5 and PM10)₱, ozone, nitrogen dioxide, sulfur dioxide and carbon monoxide., Geneva, 2021. ⟨https://apps.who.int/iris/handle/10665/345329⟩.
[3] World Health Organization, Fact Sheets: Household Air Pollution, Geneva, 2022.
[4] V.Van Tran, D. Park, Y.-C. Lee, Indoor air pollution, related human diseases, and recent trends in the control and improvement of indoor air quality, Int. J. Environ. Res. Public Health 17 (2020) 2927, https://doi.org/10.3390/ijerph17082927.
[5] P. Rybarczyk, B. Szulczyński, J. Gębicki, J. Hupka, Treatment of malodorous air in biotrickling filters: a review, Biochem. Eng. J. 141 (2019) 146–162, https://doi.org/10.1016/j.bej.2018.10.014.
[6] G. Soreanu, E. Dumont, From Biofiltration to Promising Options in Gaseous Fluxes Biotreatment, Elsevier, 2020, https://doi.org/10.1016/C2018-0-03712-3.
[7] S.K. Padhi, S. Gokhale, Treatment of gaseous volatile organic compounds using a rotating biological filter, Bioresour. Technol. 244 (2017) 270–280, https://doi.org/10.1016/j.biortech.2017.07.112.
[8] W.-T. Tsai, An overview of health hazards of volatile organic compounds regulated as indoor air pollutants, Rev. Environ. Health 34 (2019) 81–89, https://doi.org/10.1515/reveh-2018-0046.
[9] J. González-Martín, N.J.R. Kraakman, C. Pérez, R. Lebrero, R. Muñoz, A state–of–the-art review on indoor air pollution and strategies for indoor air pollution control, Chemosphere 262 (2021) 128376, https://doi.org/10.1016/j.chemosphere.2020.128376.
[10] C. Kennes, M.C. Veiga, Air Pollution Prevention and Control: Bioreactors and Bioenergy, John Wiley & Sons, 2013.
[11] D. Dobslaw, O. Ortlinghaus, Biological waste air and waste gas treatment: overview, challenges, operational efficiency, and current trends, Sustainability 12 (2020) 8577, https://doi.org/10.3390/su12208577.
[12] N.J.R. Kraakman, J. González-Martín, C. Pérez, R. Lebrero, R. Muñoz, Recent advances in biological systems for improving indoor air quality, Rev. Environ. Sci. Biotechnol. 20 (2021) 363–387, https://doi.org/10.1007/s11157-021-09569-x.
[13] R. Lebrero, D. Volckaert, R. Pérez, R. Muñoz, H. Van Langenhove, A membrane bioreactor for the simultaneous treatment of acetone, toluene, limonene and hexane at trace level concentrations, Water Res. 47 (2013) 2199–2212, https://doi.org/10.1016/j.watres.2013.01.041.
[14] N.J.R. Kraakman, J. González-Martín, C. Pérez, E. Rodríguez, R. Lebrero, M. A. Deshusses, R. Muñoz, Hydrophobic air pollutants removal at one second gas contact in a multi-channel capillary bioreactor, J. Environ. Chem. Eng. 11 (2023) 110502, https://doi.org/10.1016/j.jece.2023.110502.
[15] J.M. Estrada, G. Quijano, Bioremediation of air using microorganisms immobilized in bedding nanomaterials, Nanomater. Air Remediat (2020) 211–225, https://doi.org/10.1016/B978-0-12-818821-7.00011-7.
[16] K.V.K. Boodhoo, M.C. Flickinger, J.M. Woodley, E.A.C. Emanuelsson, Bioprocess intensification: a route to efficient and sustainable biocatalytic transformations for the future, Chem. Eng. Process. Process. Intensif. 172 (2022) 108793, https://doi.org/10.1016/j.cep.2022.108793.
[17] H. Wu, H. Yan, Y. Quan, H. Zhao, N. Jiang, C. Yin, Recent progress and perspectives in biotrickling filters for VOCs and odorous gases treatment, J. Environ. Manag. 222 (2018) 409–419, https://doi.org/10.1016/j.jenvman.2018.06.001.
[18] K.L. Dunbar, S. Hingley-Wilson, J.L. Keddie, Microbial production of hydrogen, Johns. Matthey Technol. Rev. 67 (2023) 402–413, https://doi.org/10.1595/205651323× 16806845172690.
[19] J.L. Gosse, M.C. Flickinger, Uniform Lab-Scale Biocatalytic Nanoporous Latex Coatings for Reactive Microorganisms, in: P. Wang (Ed.), Nanoscale Biocatal. (Methods Protoc, Humana Press, 2011, pp. 213–222, https://doi.org/10.1007/978-1-61779-132-1_17.
[20] M. Piskorska, T. Soule, J.L. Gosse, C. Milliken, M.C. Flickinger, G.W. Smith, C. M. Yeager, Preservation of H2 production activity in nanoporous latex coatings of RhodopseudomonaspalustrisCGA009 during dry storage at ambient temperatures, Microb. Biotechnol. 6 (2013) 515–525, https://doi.org/10.1111/1751-7915.12032.
[21] O.I. Bernal, C.B. Mooney, M.C. Flickinger, Specific photosynthetic rate enhancement by cyanobacteria coated onto paper enables engineering of highly reactive cellular biocomposite "leaves", Biotechnol. Bioeng. 111 (2014) 1993–2008, https://doi.org/10.1002/bit.25280.
[22] J.M. Estrada, O.I. Bernal, M.C. Flickinger, R. Muñoz, M.A. Deshusses, Biocatalytic coatings for air pollution control: a proof of concept study on VOC biodegradation, Biotechnol. Bioeng. 112 (2015) 263–271, https://doi.org/10.1002/bit.25353.

[23] J. González-Martín, S. Cantera, R. Muñoz, R. Lebrero, Indoor air VOCs biofiltration by bioactive coating packed bed bioreactors, J. Environ. Manag. 349 (2024) 119362, https://doi.org/10.1016/j.jenvman.2023.119362.
[24] J. González-Martín, S. Cantera, R. Lebrero, R. Muñoz, Biofiltration based on bioactive coatings for the abatement of indoor air VOCs, Sustain. Chem. Pharm. 31 (2023) 100960, https://doi.org/10.1016/j.scp.2022.100960.
[25] Y. Chen, S. Krings, J.R. Booth, S.A.F.F. Bon, S. Hingley-Wilson, J.L. Keddie, Introducing porosity in colloidal biocoatings to increase bacterial viability, Biomacromolecules 21 (2020) 4545–4558, https://doi.org/10.1021/acs.biomac.0c00649.
[26] Y. Chen, S. Krings, A.M.J.M. Beale, B. Guo, S. Hingley-Wilson, J.L. Keddie, Waterborne coatings encapsulating living nitrifying bacteria for wastewater treatment, Adv. Sustain. Syst. 6 (2022), https://doi.org/10.1002/adsu.202200312.
[27] C. Mandin, M. Trantallidi, A. Cattaneo, N. Canha, V.G. Mihucz, T. Szigeti, R. Mabilia, E. Perreca, A. Spinazzè, S. Fossati, Y. De Kluizenaar, E. Cornelissen, I. Sakellaris, D. Saraga, O. Hänninen, E. De Oliveira Fernandes, G. Ventura, P. Wolkoff, P. Carrer, J. Bartzis, Assessment of indoor air quality in office buildings across Europe – the OFFICAIR study, Sci. Total Environ. 579 (2017) 169–178, https://doi.org/10.1016/j.scitotenv.2016.10.238.
[28] D. Singh, A. Kumar, K. Kumar, B. Singh, U. Mina, B.B. Singh, V.K. Jain, Statistical modeling of O3, NOx, CO, PM2.5, VOCs and noise levels in commercial complex and associated health risk assessment in an academic institution, Sci. Total Environ. 572 (2016) 586–594, https://doi.org/10.1016/j.scitotenv.2016.08.086.
[29] T. Yamaguchi, S. Nakamura, M. Hatamoto, E. Tamura, D. Tanikawa, S. Kawakami, A. Nakamura, K. Kato, A. Nagano, T. Yamaguchi, A novel approach for toluene gas treatment using a downflow hanging sponge reactor, Appl. Microbiol. Biotechnol. 102 (2018) 5625–5634, https://doi.org/10.1007/s00253-018-8933-5.
[30] L.R. López de León, K.E. Deaton, M.A. Deshusses, Miniaturized biotrickling filters and capillary microbioreactors for process intensification of VOC treatment with intended application to indoor air, Environ. Sci. Technol. 53 (2019) 1518–1526, https://doi.org/10.1021/acs.est.8b05209.
[31] W.R. Finnerty, The biology and genetics of the Genus rhodococcus, Annu. Rev. Microbiol 46 (1992) 193–218, https://doi.org/10.1146/annurev.mi.46.100192.001205.
[32] M.J. Larkin, L.A. Kulakov, C.C.R. Allen, Biodegradation and Rhodococcus – masters of catabolic versatility, Curr. Opin. Biotechnol. 16 (2005) 282–290, https://doi.org/10.1016/j.copbio.2005.04.007.
[33] P. In-na, E.B. Sharp, G.S. Caldwell, M.G. Unthank, J.J. Perry, J.G.M.M. Lee, Engineered living photosynthetic biocomposites for intensified biological carbon capture, Sci. Rep. 12 (2022) 1–15, https://doi.org/10.1038/s41598-022-21686-3.
[34] G.S. Caldwell, P. In-Na, R. Hart, E. Sharp, A. Stefanova, M. Pickersgill, M. Walker, M. Unthank, J. Perry, J.G.M.M. Lee, Immobilising microalgae and cyanobacteria as biocomposites: new opportunities to intensify algae biotechnology and bioprocessing, Energies 14 (2021) 2566, https://doi.org/10.3390/en14092566.
[35] C. Xu, B. Frigo-Vaz, J. Goering, P. Wang, Gas-phase degradation of VOCs using supported bacteria biofilms, Biotechnol. Bioeng. 120 (2023) 1323–1333, https://doi.org/10.1002/bit.28348.
[36] J.L. Gosse, M.S. Chinn, A.M. Grunden, O.I. Bernal, J.S. Jenkins, C. Yeager, S. Kosourov, M. Seibert, M.C. Flickinger, A versatile method for preparation of hydrated microbial-latex biocatalytic coatings for gas absorption and gas evolution, J. Ind. Microbiol. Biotechnol. 39 (2012) 1269–1278, https://doi.org/10.1007/s10295-012-1135-8.
[37] M.J. Schulte, J. Wiltgen, J. Ritter, C.B. Mooney, M.C. Flickinger, P. Way, N. Carolina, N. Carolina, A high gas fraction, reduced power, syngas bioprocessing method demonstrated with a Clostridium ljungdahlii OTA1 paper biocomposite, Biotechnol. Bioeng. 113 (2016) 1913–1923, https://doi.org/10.1002/bit.25966.
[38] M. Ferdowsi, A. Avalos Ramirez, J.P. Jones, M. Heitz, Elimination of mass transfer and kinetic limited organic pollutants in biofilters: a review, Int. Biodeterior. Biodegrad. 119 (2017) 336–348, https://doi.org/10.1016/j.ibiod.2016.10.015.
[39] O.K. Lyngberg, C.P. Ng, V. Thiagarajan, L.E. Scriven, M.C. Flickinger, Engineering the microstructure and permeability of thin multilayer latex biocatalytic coatings containing E. coli, Biotechnol. Prog. 17 (2001) 1169–1179, https://doi.org/10.1021/bp0100979.
[40] C. Yang, G. Yu, G. Zeng, H. Yang, F. Chen, C. Jin, Performance of biotrickling filters packed with structured or cubic polyurethane sponges for VOC removal, J. Environ. Sci. 23 (2011) 1325–1333, https://doi.org/10.1016/S1001-0742(10)60565-7.
[41] H. Wu, C. Guo, Z. Yin, Y. Quan, C. Yin, Performance and bacterial diversity of biotrickling filters filled with conductive packing material for the treatment of toluene, Bioresour. Technol. 257 (2018) 201–209, https://doi.org/10.1016/j.biortech.2018.02.108.
[42] Z. Zhang, Y. Zhou, X. Zhu, L. Fei, H. Huang, Y. Wang, Applications of ESEM on materials science: recent updates and a look forward, Small Methods 4 (2020) 1900588, https://doi.org/10.1002/smtd.201900588.
[43] M. Alhede, K. Qvortrup, R. Liebrechts, N. Høiby, M. Givskov, T. Bjarnsholt, Combination of microscopic techniques reveals a comprehensive visual impression of biofilm structure and composition, FEMS Immunol. Med. Microbiol 65 (2012) 335–342, https://doi.org/10.1111/j.1574-695X.2012.00956.x.
[44] L. Muscariello, F. Rosso, G. Marino, A. Giordano, M. Barbarisi, G. Cafiero, A. Barbarisi, A critical overview of ESEM applications in the biological field, J. Cell. Physiol. 205 (2005) 328–334, https://doi.org/10.1002/jcp.20444.
[45] R. Aston, K. Sewell, T. Klein, G. Lawrie, L. Grøndahl, Evaluation of the impact of freezing preparation techniques on the characterisation of alginate hydrogels by cryo-SEM, Eur. Polym. J. 82 (2016) 1–15, https://doi.org/10.1016/j.eurpolymj.2016.06.025.
[46] A. Bridier, T. Meylheuc, R. Briandet, Realistic representation of Bacillus subtilis biofilms architecture using combined microscopy (CLSM, ESEM and FESEM), Micron 48 (2013) 65–69, https://doi.org/10.1016/j.micron.2013.02.013.
[47] J. Qiao, J. Adams, D. Johannsmann, Addition of halloysite nanotubes prevents cracking in drying latex films, Langmuir 28 (2012) 8674–8680, https://doi.org/10.1021/la3011597.